Geophys. J. Int. (1998) **133,** F7–F10

FAST-TRACK PAPER

Seismic image of a CO_2 reservoir beneath a seismically active volcano

Bruce R. Julian,[1] A. M. Pitt[1] and G. R. Foulger[2]

[1] *US Geological Survey,* 345 *Middlefield Road* MS977, *Menlo Park,* 94025 CA, *USA. E-mail: julian@andreas.wr.usgs.gov*
[2] *Department of Geological Sciences, University of Durham, Durham,* DH1 3LE, *UK*

Accepted 1998 January 15. Received 1998 January 8; in original form 1997 September 30

SUMMARY

Mammoth Mountain is a seismically active volcano 200 000 to 50 000 years old, situated on the southwestern rim of Long Valley caldera, California. Since 1989 it has shown evidence of unrest in the form of earthquake swarms (Hill *et al.* 1990), volcanic 'long-period' earthquakes (Pitt & Hill 1994), increased output of magmatic ^{3}He (Sorey *et al.* 1993) and the emission of about 500 tonnes day^{-1} of CO_2 (Farrar *et al.* 1995; Hill 1996; M. Sorey, personal communication, 1997), which has killed trees and poses a threat to human safety. Local-earthquake tomography shows that in mid-1989 areas of subsequent tree-kill were underlain by extensive regions where the ratio of the compressional and shear elastic-wave speeds V_P/V_S was about 9 per cent lower than in the surrounding rocks. Theory (Mavko & Mukerji 1995), experiment (Ito, DeVilbiss & Nur 1979), and experience at other geothermal/volcanic areas (Julian *et al.* 1996) and at petroleum reservoirs (Harris *et al.* 1996) indicate that V_P/V_S is sensitive to pore-fluid compressibility, through its effect on V_P. The observed V_P/V_S anomaly is probably caused directly by CO_2, and seismic V_P/V_S tomography is thus a promising tool for monitoring gas concentration and movement in volcanoes, which may in turn be related to volcanic activity.

Key words: earthquake, gas, seismology, structure, tomography, volcano.

THE DATA

We determined the 3-D seismic-wave structure near Mammoth Mountain using 2480 P and 1489 $S-P$ times from 289 local earthquakes that occurred between June 1989 and July 1990. The earthquakes were part of a swarm that began in May 1989 and was probably caused by a magmatic intrusion (Hill *et al.* 1990) (Figs 1 and 2). The earthquakes were recorded on 10 1-Hz vertical-component seismometers (Mark Products model L-4) of the US Geological Survey's Northern California Seismic Network (NCSN) (Fig. 1), which supplied 1852 P and 909 $S-P$ times. In addition, 12 three-component 2-Hz sensors (Mark Products model L-22) using GEOS digital data loggers (Borcherdt *et al.* 1985) were deployed for four days in June 1989 and supplied 628 P and 580 $S-P$ times from 116 of the events. We measured arrival times from digital seismograms sampled at intervals of 0.01 s (NCSN) and 0.005 s (temporary network). The measured times are precise to about 0.01 s.

With NCSN data, S phases had to be measured from vertical-component seismograms, so there are only about half as many measured S phases per P phase as there are from the temporary three-component network. Agreement between times from co-located and closely spaced instruments indicates that S times measured using vertical instruments are accurate to about 0.05 s. The errors are caused primarily by near-receiver S-to-P mode conversion, and are largely independent of earthquake location, so these observations are more useful in seismic tomography than the formal accuracy suggests.

THE TOMOGRAPHY

The tomography algorithm (Evans, Eberhart-Phillips & Thurber 1994) uses an iterative damped least-squares method to invert the observed arrival times, simultaneously estimating the locations of the earthquakes, the ray paths and the 3-D V_P and V_P/V_S fields, which are parametrized by values at the nodes of a 3-D rectangular grid. Trilinear interpolation is used to evaluate V_P and V_P/V_S between the nodes. Our grid covers a 12×8 km area and extends from the surface (about 2.7 km above sea level) to 8 km below sea level. The grid spacing is 2 km horizontally and 1 km vertically. The final model reduces the variance of P time residuals by 66 per cent and $S-P$ residuals by 54 per cent, with respect to the initial

GJI000 2/4/98 07:59:19 3B2 version 5.20
The Charlesworth Group, Huddersfield 01484 517077

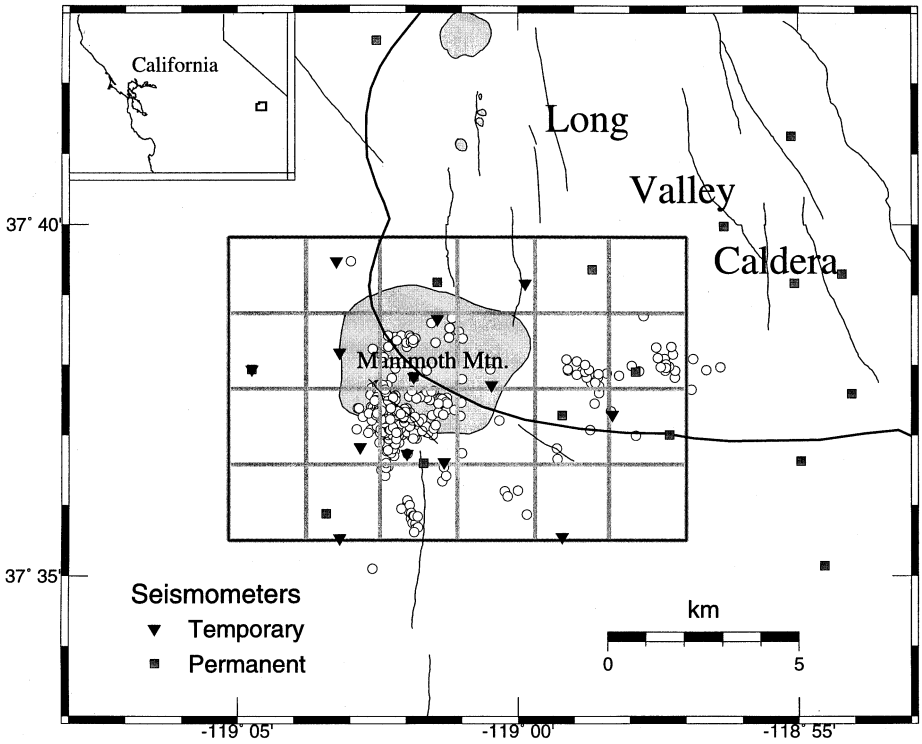

Figure 1. Map of Mammoth Mountain area. Heavy line: boundary of Long Valley caldera; thin lines: other faults; grey areas: Mammoth Mountain and the recent (~500 a) eruptives of the Inyo domes and craters. White circles: the 289 earthquakes used in this study; triangles: three-component digital seismometers operated for four days in June 1989; squares: permanent (mostly vertical-component) seismometers of the USGS. Black rectangle: 12×8 km area of the 3-D model; grey lines: 2-km grid on which V_P and V_P/V_S fields are defined. The vertical grid spacing is 1 km.

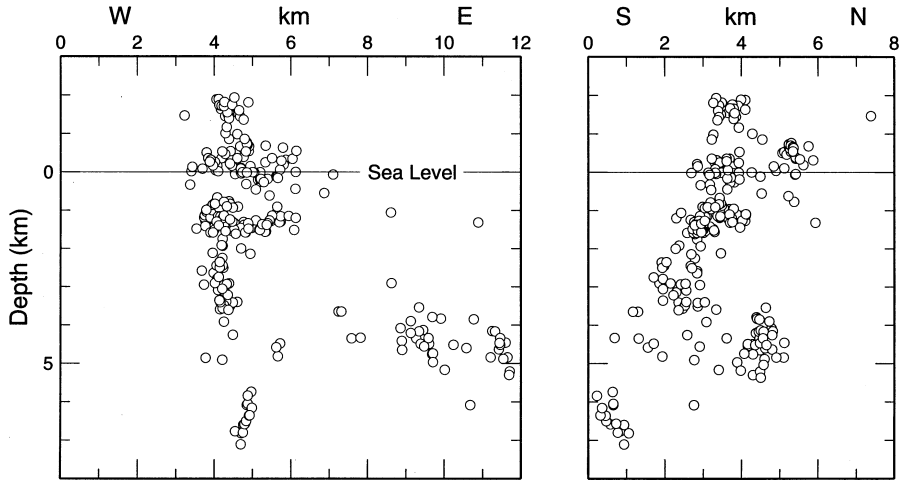

Figure 2. West–east and south–north cross-sections showing the 289 earthquakes used in this study. Vertical boundaries correspond to the limits of the 3-D model (Fig. 1).

1-D model (Table 1), which was obtained by inverting a regional local-earthquake data set (E. Kissling, personal communication, 1996). The final RMS time residual is 0.036 s for P and 0.080 s for $S-P$.

RESULTS

The derived compressional-wave-speed V_P field (Fig. 3) generally reflects known geological structure. At shallow

Figure 3. Compressional-wave speed V_P (left) and wave-speed ratio V_P/V_S (right) at four depths. Heavy line: boundary of Long Valley caldera; light line: outline of Mammoth Mountain. Wave speed is lower in the caldera than in crystalline rocks of the Sierra Nevada to the south and west, and is also low near Holocene cinder cones southwest of Mammoth Mountain. A small region with anomalously low V_P/V_S below sea level on the southeast side of Mammoth Mountain spreads at shallower depths and separates into two separate areas near the surface. White areas: places where trees have been killed by CO_2 emissions since 1989 (courtesy of Water Resources Division, USGS). These areas are controlled locally by fissures and faults, but they generally occur above the margins of regions where V_P/V_S at shallow depths is low.

GJI000 2/4/98 07:59:41 3B2 version 5.20
The Charlesworth Group, Huddersfield 01484 517077

Table 1. Starting model used for the inversion.

Depth to top of layer, km	*P*-wave speed, km s^{-1}
−4.0	3.00
−2.0	3.55
−1.0	4.45
0.0	5.35
1.0	5.56
2.0	5.78
3.0	5.87
4.0	5.96
5.0	6.00
6.0	6.04
7.0	6.06
8.0	6.07
10.0	6.08
V_P/V_S ratio	1.67

depths V_P is about 30 per cent lower in the Bishop tuff that fills Long Valley caldera than in the surrounding crystalline rocks of the Sierra Nevada. The caldera rim is marked by a positive V_P anomaly except at the edifice of Mammoth Mountain. A negative anomaly of about 12 per cent occurs southwest of Mammoth Mountain near Red Cones, a pair of Holocene basaltic cinder cones, and suggests high temperatures or the presence of magma there.

In contrast, the wave-speed ratio V_P/V_S shows strong variations that are not related so obviously to local geology (Fig. 3). A strong negative V_P/V_S anomaly [$\Delta(V_P/V_S) \approx -0.15$, or 9 per cent] underlies Mammoth Mountain down to at least 1 km below sea level, and has a shape that suggests the path of an upward-migrating fluid. It is most compact below sea level, widens at shallower depths, and near the surface separates into two parts. At depths greater than 2 km below sea level, the V_P/V_S anomaly may connect with a volume of low V_P/V_S and high *P*-wave attenuation to the east of Mammoth Mountain imaged in a recent regional study (Sanders *et al.* 1995), but our network is too small to verify this or to rule this out.

DISCUSSION

The V_P/V_S anomaly is probably caused by gaseous pore fluid. Both elasticity theory (Mavko & Mukerji 1995) and laboratory experiments (Ito *et al.* 1979) indicate that V_P/V_S in porous rocks is sensitive to pore-fluid compressibility, with gases causing the strongest effect. Negative V_P/V_S anomalies are known from other geothermal and volcanic regions, including Yellowstone, WY (Chaterjee, Pitt & Iyer 1985), Coso, CA (Walck 1988), Hengill–Grensdalur, Iceland (Foulger *et al.* 1995) and The Geysers, CA (O'Connell 1986; Julian *et al.* 1996). These areas all have liquid-dominated geothermal systems except for The Geysers (a steam field), and only The Geysers has a V_P/V_S anomaly as strong as that at Mammoth Mountain. Furthermore, industrial flooding of hydrocarbon reservoirs with CO_2 has been known to decrease V_P by nearly 20 per cent, as determined by cross-hole seismic tomography and well logging (Harris *et al.* 1996). This effect increases with porosity, so a 9 per cent V_P/V_S anomaly such as that at Mammoth Mountain clearly could be caused by CO_2 bodies in the porous rocks typical of volcanoes.

The location of the V_P/V_S anomaly is consistent with it being the source of the ongoing CO_2 emissions that have killed trees since the 1989 earthquake swarm (Fig. 3). The strongest CO_2 emissions, as judged by areas of tree-kill, occur above the edges of the V_P/V_S anomaly. Such a geometric relation is expected from elasticity theory. Around a pressurized reservoir, the highest hoop stresses, and thus the region of easiest fracture breakout and gas escape, occur on the circle of tangency with a cone whose apex is at the free surface (McTigue 1987). The anomaly cannot, on the other hand, have originated suddenly in 1989 because the required rapid expulsion of water from ~ 20 km^3 of rock (the approximate volume of the V_P/V_S anomaly in Fig. 3) would have produced strong hydrological and geodetic effects that were not observed, despite intensive monitoring in the area. It is more likely that magmatic activity in 1989 both caused the earthquake swarm and activated a CO_2 reservoir that is either a permanent feature of the volcano or accumulated over a long period of time prior to 1989. In that case, CO_2 may be flowing into the reservoir from a deeper source at approximately the same rate as it is venting from the surface. Evidence in support of such flow has recently been found by Cramer & McNutt (1997), who identified 'long-period' earthquake activity, usually attributed to unsteady fluid advection, 1.5 to 3.5 km below sea level in the 1989 Mammoth Mountain earthquake swarm. A deep magmatic source for the CO_2 is indicated by both Helium isotope ratios (Sorey *et al.* 1993) and the locations of earthquakes (Hill *et al.* 1990). A diffuse zone of long-period earthquakes to the SW of Mammoth Mountain, with hypocentral depths of up to about 20 km, correlates temporally with the outgassing of the CO_2, suggesting a mid-crustal or mantle location for this deeper source. If inflow exceeds or falls short of outflow, the reservoir will have changed in volume since 1989. Repeated tomographic studies have recently been shown to be capable of detecting such reservoir changes at The Geysers (Foulger *et al.* 1997). In view of the current state of activation of Mammoth Mountain, and the common association of gas emissions and eruptions, there is thus a strong case for repeated tomographic study of this and other active volcanoes.

ACKNOWLEDGMENTS

We thank Phillip Dawson and Harley Benz for critical reviews of the manuscript and John Evans for helpful discussions. Any use of trade, firm or product names and trademarks in this publication is for descriptive purposes only and does not constitute endorsement by the US Government.

REFERENCES

Borcherdt, R.D. *et al.*, 1985. A general earthquake-observation system (GEOS), *Bull. seism. Soc. Am.,* **75,** 1783–1825.

Chaterjee, S.N., Pitt, A.M. & Iyer, H.M., 1985. V_P/V_S ratios in the Yellowstone National Park region, Wyoming, *J. Volc. Geotherm. Res.,* **26,** 213–230.

Cramer, C.H. & McNutt, S.R., 1997. Spectral analysis of earthquakes in the 1989 Mammoth Mountain swarm near Long Valley, California, *Bull. seism. Soc. Am.,* **89,** 1454–1462.

Evans, J.R., Eberhart-Phillips, D. & Thurber, C.H., 1994. User's manual for SIMULPS12 for imaging V_P and V_P/V_S, a derivative of the Thurber tomographic inversion SIMUL3 for local earthquakes and explosions, *US Geol. Surv. Open-file Rept,* **94–431**.

GJI000 2/4/98 07:59:57 3B2 version 5.20
The Charlesworth Group, Huddersfield 01484 517077

Farrar, C.D., Sorey, M.L., Evans, W.C., Howle, J.F., Kerr, B.D., Kennedy, B.M., King, C.-Y. & Southon, J.R., 1995. Forest-killing diffuse CO_2 emission at Mammoth Mountain as a sign of magmatic unrest, *Nature,* **376,** 675–678.

Foulger, G.R., Miller, A.D., Julian, B.R. & Evans, J.R., 1995. Three-dimensional v_P and v_P/v_S structure of the Hengill triple junction and geothermal area, Iceland, and the repeatability of tomographic inversion, *Geophys. Res. Lett.,* **22,** 1309–1312.

Foulger, G.R., Grant, C.C., Ross, A. & Julian, B.R., 1997. Industrially induced changes in Earth structure at The Geysers geothermal area, California, *Geophys. Res. Lett.,* **97,** 135–137.

Harris, J.M., Langan, R.T., Fasnacht, T., Melton, D., Smith, B. & Sinton, F., 1996. Experimental verification of seismic monitoring of CO_2 injection in carbonate reservoirs, *Soc. expl. Geophys. Tech. Program* 1870–1872.

Hill, D.P. *et al.,* 1990. The 1989 earthquake swarm beneath Mammoth Mountain, California: an initial look at the 4 May through 30 September activity, *Bull. seism. Soc. Am.,* **80,** 325–339.

Hill, D.P., 1996. Earthquakes and carbon dioxide beneath Mammoth Mountain, California, *Seism. Res. Lett.,* **67,** 8–15.

Ito, H., DeVilbiss, J. & Nur, A., 1979. Compressional and shear waves in saturated rock during water-steam transition, *J. geophys. Res.,* **84,** 4731–4735.

Julian, B.R., Ross, A., Foulger, G.R. & Evans, J.R., 1996. Three-dimensional seismic image of a geothermal reservoir: The Geysers, California, *Geophys. Res. Lett.,* **23,** 685–688.

Mavko, G. & Mukerji, T., 1995. Seismic pore space compressibiliby and Gassman's relation, *Geophysics*, **60,** 1743–1749.

McTigue, D.F., 1987. Elastic stress and deformation near a finite spherical magma body: resolution of the point source paradox, *J. geophys. Res.,* **92,** 12 931–12 940.

O'Connell, D.R., 1986. Seismic velocity structure and microearthquake properties at The Geysers, California geothermal area, *PhD thesis,* University of California, Berkeley, CA.

Pitt, A.M. & Hill, D.P., 1994. Long-period earthquakes in the Long Valley caldera region, eastern California, *Geophys. Res. Lett.,* **21,** 1679–1682.

Sanders, C.O., Ponko, S.C., Nixon, L.D. & Schwartz, E.A., 1995. Seismological evidence for magmatic and hydrothermal structure in Long Valley caldera from local earthquake attenuation and velocity tomography, *J. geophys. Res.,* **100,** 8311–8326.

Sorey, M.L., Kennedy, B.M., Evans, W.C., Farrar, C.D. & Suemnicht, G.A., 1993. Heluim isotope and gas discharge variations associated with crustal unrest in Long Valley caldera, California, 1989-1992, *J. geophys. Res.,* **98,** 15 871–15 889.

Walck, M.C., 1988. Three-dimensional V_P/V_S variations for the Coso region, California, *J. geophys. Res.,* **93,** 2047–2052.

GJI000 2/4/98 08:00:11 3B2 version 5.20
The Charlesworth Group, Huddersfield 01484 517077

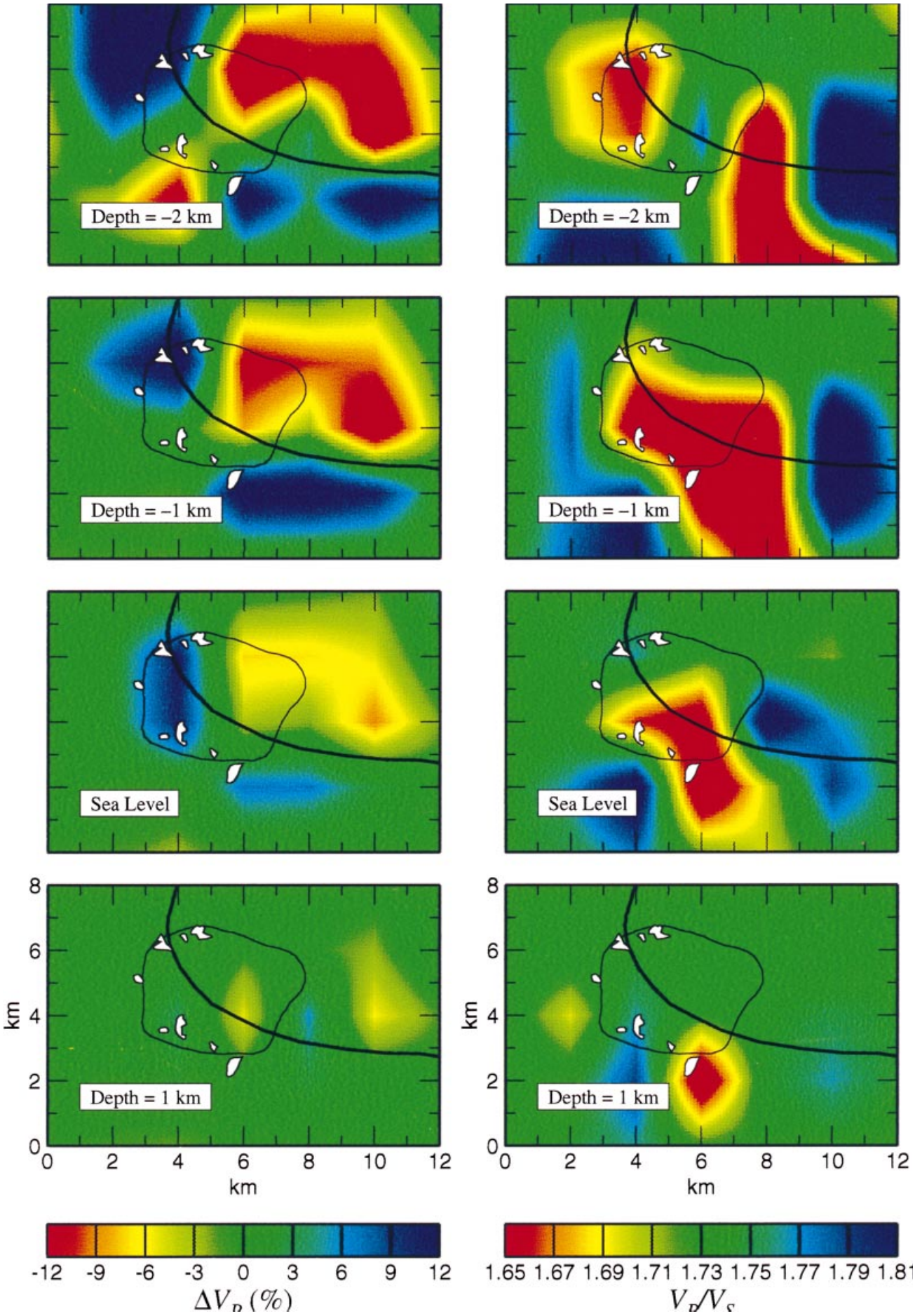

GJI000 2/4/98 08:00:22 3B2 version 5.20
The Charlesworth Group, Huddersfield 01484 517077

Opposite p.F8